Enter: Journal or Event Name

Enter: Paper Number (SPE-123456) or Manuscript ID

Green Acid Technology for Carbonate Reservoirs in Kuwait: A Sustainable Approach to Reservoir Stimulation and Management

Haithm Salah Hagar[1,2], Jyun-Syung Tsau[1,2], Stephen Rowley[3], Mubarak Alhajeri and Reza Barati[1,2*]

[1]University of Kansas, Tertiary Oil Recovery Program (TORP), Lawrence, KS, USA
[2]University of Kansas, Chemical and Petroleum Engineering Department, Lawrence, KS, USA
[3] Heartland Energy Group Ltd, Grain Valley, MO, USA

Abstract

This study evaluates the performance of a synthetic green-acid system (Oil Safe AR®) as an environmentally friendly alternative to hydrochloric acid (HCl) for matrix acidizing in carbonate formations. A comprehensive experimental program was performed, including single-core and dual-core coreflooding tests conducted under low-temperature (40 °C) and high-temperature (82 °C) conditions, followed by analysis of multi-well field treatments. In laboratory tests, the green acid (Oil Safe AR®) consistently demonstrated moderated reaction kinetics that promoted deeper acid penetration and more uniform wormhole development compared with conventional 15 wt% HCl. Dual-core experiments showed that green acid (Oil Safe AR®) achieved stable and sustained diversion at both low and high temperatures when injected above a critical flow rate, whereas HCl produced only transient diversion dominated by rapid face dissolution. Core-scale results were in strong agreement with field treatments, where the green-acid system (Oil Safe AR®) delivered significant and persistent improvements in production and injectivity. Overall, the findings demonstrate that green acid (Oil Safe AR®) provides a safer and more controlled stimulation option, especially in carbonate reservoirs where conventional HCl tends to react too aggressively and unpredictably.

Introduction

Hydrocarbon-based energy (fossil fuel) remains the dominant primary energy source worldwide, currently satisfying roughly 80–85 % of global energy demand (Hagar and Foroozesh 2021; Hagar et al. 2022). The multiple advantages of hydrocarbons including low production cost, mature extraction technologies, well-established distribution networks, and widespread availability, have made them vital to the functioning of the global economy. Despite accelerating efforts toward renewable integration, forecasts from the International Energy Agency (International Energy Agency (IEA) 2019) indicate that global energy consumption is expected to nearly double by 2050, driven by industrial growth, urbanization, and population increase. Consequently, the sustained contribution of oil reservoirs to the world's energy supply remains critical. Improving the efficiency of hydrocarbon recovery and ensuring the long-term productivity of mature fields therefore constitute central technical and economic priorities for petroleum engineers (Ali and Nasr-El-Din 2020; Mahmoud et al. 2021). Among various stimulation and enhanced recovery methods, matrix acidizing has proven to be one of the most effective techniques for restoring near-wellbore permeability and improving hydrocarbon productivity in carbonate reservoirs (Alameen et al. 2023, 2024; Hagar et al. 2024; Mohsin Yousufi et al. 2025).

Matrix acidizing continues to serve as a primary stimulation method in carbonate reservoirs, where productivity losses often arise from drilling-induced damage, fines migration, scale deposition, and heterogeneity (Ali et al. 2020). Hydrochloric acid (HCl) remains the industry standard for carbonate stimulation due to its strong and instantaneous reaction with $CaCO_3$, enabling rapid dissolution and the formation of wormholes that enhance near-wellbore conductivity (Bazin 2001; Golfier et al. 2002). However, these same characteristics present significant challenges. The rapid reaction rate of HCl leads to near-instantaneous surface spending, limiting penetration depth and increasing the likelihood of face dissolution rather than deep, conductive wormhole development. At elevated temperatures, these issues are amplified, as HCl becomes even more reactive, promoting uncontrolled etching, wormhole instability, and difficulty in achieving reliable diversion (Dong 2018; Aljawad et al. 2021). In heterogeneous formations, acids preferentially enter higher-permeability pathways, bypassing the tighter or more damaged zones that require treatment the most (Markey et al. 2014; Al-Ghamdi et al. 2014; Alhubail et al. 2020). These challenges underscore the need for more controlled-reactivity acid systems capable of deeper penetration, moderated dissolution, and improved flow redistribution.

Among the alternatives to HCl, green acids (Oil Safe AR®) have gained increasing attention due to their moderated reaction kinetics, reduced corrosion potential, and improved thermal stability (Maheshwari et al. 2016; Barati Ghahfarokhi and Alhubail 2021; Zhu et al. 2022). These formulations are designed to deliver the benefits of acid stimulation while minimizing the drawbacks of overly aggressive reactivity. Unlike viscoelastic diverting acids or surfactant-thickened systems, which rely on in-situ viscosity development or micelle structuring, green acids (Oil Safe AR®) achieve controlled stimulation primarily through moderated proton release and reduced surface reaction rates (Al-Ghamdi et al. 2014; Liu and Liu 2016; Barboza et al. 2022). This enables deeper acid penetration, smoother dissolution fronts, and a more uniform propagation of wormholes—attributes that are particularly advantageous in high-temperature carbonate conditions where HCl reacts too rapidly to maintain live acid transport (Zhang et al. 2021; Cao et al. 2021b). Previous laboratory studies have shown that moderated-reactivity acids can enhance breakthrough efficiency and reduce undesired face dissolution compared with HCl. However, only limited research has systematically evaluated their diversion behavior, especially in controlled parallel-core configurations that simulate heterogeneity in a quantifiable manner.

Achieving effective diversion remains one of the most persistent challenges in carbonate stimulation, as acid flow naturally favors high-permeability pathways, leaving low-permeability or damaged intervals untreated (Maheshwari et al. 2016). Dual core coreflooding provides a powerful laboratory technique for studying diversion because it allows direct monitoring of flow distribution between contrasting permeability channels under identical injection conditions(Al-Ghamdi et al. 2014; Cao et al. 2021a). This approach enables clear differentiation between acid systems in terms of pressure behavior, breakthrough characteristics, and wormhole propagation (Dong 2018; Hagar et al. 2020, 2023, 2025; Liu et al. 2021). In high-temperature carbonate reservoirs, diversion becomes even more difficult due to rapid reaction kinetics and increased CO_2 evolution, which can disrupt pressure balance and accelerate pore-scale instabilities (Ma et al. 2018; Liu et al. 2021; Mustafa et al. 2021). The present study addresses this knowledge gap by evaluating the performance of a green-acid system (Oil Safe AR®) through coordinated low- and high-temperature single-core and dual-core experiments, followed by field-scale validation (Nawik et al. 2016; Alhubail et al. 2017; Barati Ghahgarokhi et al. 2024). By comparing green acid (Oil safe AR®) with 15 wt% HCl under controlled laboratory conditions, this work provides a comprehensive assessment of dissolution behavior, diversion effectiveness, and operational applicability. The integration of laboratory data with field observations strengthens the argument that green-acid (Oil Safe AR®) formulations represent a viable, safer, and more predictable alternative for matrix acidizing in carbonate reservoirs.

2. Material and Methods

2.1 Core samples and Characterization

Limestone core plugs were collected from a Kansas carbonate reservoir at depths between 4661.7 ft and 4678.3 ft, representing the lithology of a typical oil-bearing interval in the region. The cores were machined to a standard geometry of 1.0 in diameter and 2.5–2.8 in length, ensuring uniform flow geometry for comparison among the various acid systems. Each plug was first cleaned with isopropanol, oven-dried at 60 °C until constant mass and visually inspected to confirm the absence of cracks or vugs. X-ray diffraction (XRD) confirmed a dominant calcite composition of ≈ 97 wt% $CaCO_3$ with minor quartz and dolomite (< 3%), indicating a mineralogically pure limestone in which dissolution is controlled primarily by the calcite acid reaction (see appendix A). Porosity was determined using two approaches, the saturation method and nuclear magnetic resonance (NMR). Permeability measurements were performed using brine collected from the producer well. The measured porosity values ranged from 13 to 28% (average ≈ 20%), while brine-permeability tests yielded permeability values between 0.3 and 13 md, indicating tight to moderately permeable carbonate rock. Bulk volumes were typically 24–37 cm^3 with corresponding pore volumes of 5–8 mL, parameters later used to normalize pressure profiles and calculate pore-volume-injected (PVI) data.

Table 1 Physical Properties of Kansas Limestone Cores Used in the Study

No	Length	Mass dry(g)	Mass sat. (g)	Saturation Porosity (%)	NMR Porosity (%)	K (md)
1	1.8	49.44	54.95	20.47%	22.80%	3.62
2	2.71	68.54	76.31	19.18%	19.40%	2.31
12	2.41	73.13	78.12	13.84%	15.20%	2.89
13	2.36	73.08	77.72	13.05%	15.00%	4.75
14	2.57	76.66	82.54	15.30%	15.40%	0.70
17	2.74	76.74	83.13	15.60%	17.80%	2.76
19	2.48	69.08	76.91	21.11%	21.00%	7.1
21	2.5	68.76	76.92	21.80%	21.70%	2.13

For the diversion tests, two core sets were selected to provide a measurable contrast in flow capacity: Core 19-21 and Core 2-14 md), producing a permeability ratio of ~6.5:1, which lies within the effective diversion range reported for -surfactant. Other representative plugs (Cores 13,17,12 and 1) were used for single-core acid-flooding experiments to examine the influence of acid strength 7.5 %, 15

%, and 28 wt% HCl—and the green-acid (Oil Safe AR®) formulation. Table 1 summarizes the essential physical properties of all cores employed in the study. Together, these data form a consistent dataset that captures the mineralogical purity and petrophysical variability of the Kansas carbonate system investigated.

2.2 Experimental Conditions

All flooding experiments were conducted at 40 and 80 °C and 1400 psi back pressure to replicate the formation conditions of the Kansas reservoir. A thermostatically controlled stainless-steel core holder equipped with radial confinement maintained uniform temperature and pressure throughout the tests. Nitrogen-pressurized accumulators regulated back-pressures to ensure complete dissolution of the CO_2 produced during the acid–carbonate reaction, thus preventing gas-phase formation that could distort flow readings. Differential pressures across the cores were continuously recorded by high-accuracy transducers with measurement ranges of 0–300 psi for single-core and 0–350 psi for dual-core runs. Prior to acid injection, the cores were saturated under vacuum with formation brine supplied directly by the operating company, rather than synthetic brine, to reproduce authentic ionic composition and scaling tendencies. This brine was also used for permeability measurements and post-acid flushing, guaranteeing full chemical compatibility between the test fluids and the rock mineralogy. All acid solutions contained 0.5 wt % corrosion inhibitor (a methanol–amide–quaternary-ammonium blend) to prevent metallic corrosion of the injection lines and stainless-steel core holder during prolonged acid exposure. Throughout each run, effluent samples were collected in sealed glass vials for subsequent analysis of calcium concentration and pH evolution.

2.3 Acid Systems and Experimental Procedure for single core

Single-core acidizing experiments were performed under both low-temperature and high-temperature conditions to characterize the dissolution behavior, reaction kinetics, and wormhole propagation mechanisms of the green-acid formulations (Oil Safe AR 1030, 1050, and 1060®) and a series of mineral acid systems at different concentrations. The HCl systems evaluated in this study included 7.5 wt%, 10 wt%, and 15 wt% HCl, enabling comparison of controlled-reactivity acids against conventional fast-reacting formulations across a range of acid strengths.All limestone cores were dried, vacuum-saturated with brine, mounted in a stainless-steel Hassler-type core holder, and subjected to a confining pressure of 2000–2500 psi depending on test temperature. Baseline permeability was established under steady-state brine flow prior to acid injection. Low-temperature single-core tests were conducted at 40 °C with a 1400 psi back-pressure regulator, while high-temperature single-core tests were carried out at 82 °C under a 1200 psi system pressure to prevent CO_2 breakout and maintain single-phase flow.

For all single-core experiments, the acid systems were injected at a constant flow rate of 4 cm^3/min, and differential pressure across the core was recorded continuously. Wormhole breakthrough was identified by a characteristic sharp pressure drop, after which acid injection was stopped and the core was flushed with brine to determine regained permeability. The measured parameters included the injected pore volume, breakthrough pore volume, and the permeability-enhancement ratio (k_final/k_initial). Additionally, pre- and post-acidizing photographs of the inlet and outlet faces were collected for every test to evaluate the spatial morphology of dissolution, the development of wormholes, and face-etching patterns. This combined single-core methodology provided a unified framework for comparing the performance of moderated-reactivity green acids (Oil Safe AR®) with multiple concentrations of conventional HCl under both low- and high-temperature conditions.

2.4 Dual-Core Coreflooding tests

High-temperature dual-core coreflooding experiments were conducted to evaluate diversion behavior for the green-acid (Oil Safe AR®) formulation and 15 wt% HCl under thermally accelerated carbonate reaction conditions. Each experiment used two limestone cores mounted in parallel, consisting of one high-permeability and one low-permeability plug with initial permeability contrasts between 7.4 and 7.7. All tests were carried out at 82 °C, 1200 psi system pressure, and 2000 psi confining pressure, and a constant injection rate of 4 cm^3/min was applied, as this rate produced confirmed diversion for both acids. Acid injection continued until breakthrough, typically between 1.5 and 2.5 pore volumes, while differential pressure across each core was recorded continuously to quantify flow redistribution, resistance development, and wormhole breakthrough. After breakthrough, brine injection was resumed to determine regained permeability. Only two experiments exhibiting clear diversion were included in the final analysis: the 1060 green-acid (Oil Safe AR®) test (Test 6–H30) and the 15 wt% HCl test (Test 4–H4).

3. Results and Discussion

3.1 Single-Coreflood Experiments

3.1.1 Propagation of Regular and Green Acids (Oil Safe AR®) in Limestone Cores at low temperature

A series of single coreflood experiments were conducted to investigate the dissolution behavior of regular hydrochloric acids and an environmentally friendly “green acid” (Oil Safe AR®) under reservoir-relevant conditions representative of the Kansas carbonate formation (97% $CaCO_3$, 40 °C, 1400 psi). All tests were performed at a constant injection rate of 4 cm^3/min using limestone cores

approximately 1 in. in diameter and 2.4–2.8 in. in length. Brine collected from the field well, containing its native salinity and supplemented with 0.3 vol% corrosion inhibitor, was used for initial core saturation and subsequent post-acid flushing. Core characteristics, including porosity and permeability, are summarized in Table 2. The selected cores exhibited moderate porosity (13–20%) and low to intermediate permeability (2.7–4.8 md), which allowed evaluation of reaction-controlled versus diffusion-controlled regimes. Before acid injection, each core was flooded with brine until steady-state pressure was achieved to ensure complete saturation. The differential pressure (ΔP) was continuously recorded across the core as the acid was injected, followed by a brine chase to displace the remaining acid and observe post-reaction permeability changes. The normalized pressure response (ΔP_{max} / ΔP_0) was plotted against injected pore volume (PV) for each acid system (Figures 1-3). The pore volume to breakthrough (PVbt) was determined at the point where the normalized pressure dropped to zero, corresponding to the formation of a continuous flow channel or wormhole.

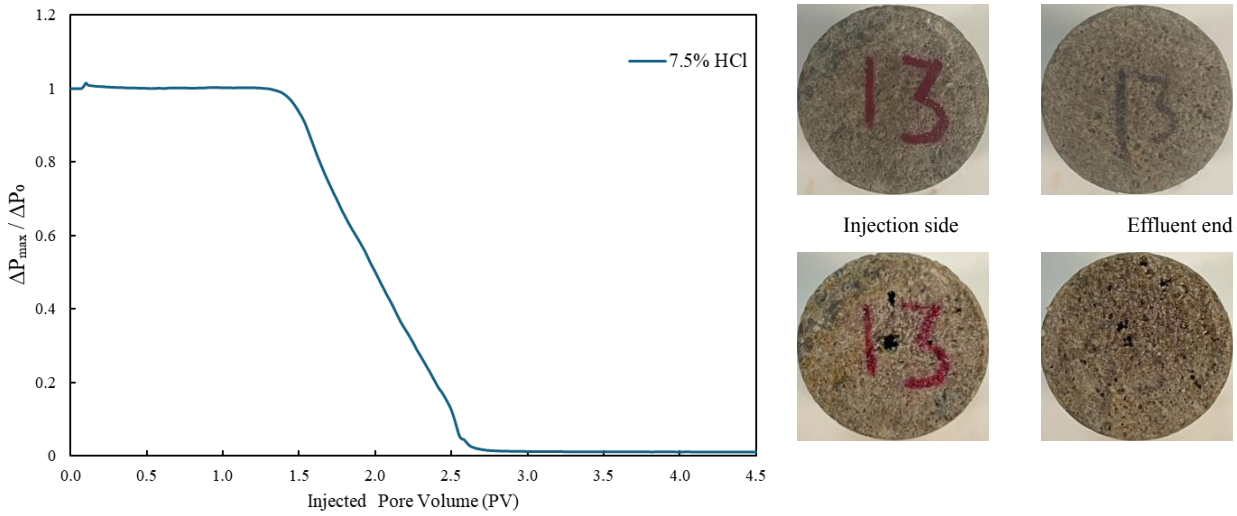

Fig. 1—Normalized differential pressure (ΔP□ax/ΔP0) versus injected pore volume for 7.5% HCl and corresponding core-end images before and after acidizing.

The injection of 7.5% HCl (Core 13) exhibited a gradual pressure decline with breakthrough occurring at 2.55 PV (Figure 1). The normalized pressure remained nearly constant for the first 1.5 PV, suggesting slow reaction kinetics and uniform front propagation. The steady ΔP profile and delayed breakthrough indicate a reaction-limited dissolution regime where acid consumption was moderate, allowing sufficient penetration depth before wormhole coalescence. The effluent brine analysis and post-test photographs revealed a smooth dissolution face with minimal channel branching, typical of efficient, uniform wormhole structures. This behavior demonstrates that low-strength acids at the tested rate can achieve controlled dissolution without premature face dissolution. In contrast, 15% HCl (Core 17) displayed a sharp decline in normalized pressure with breakthrough at 1.48 PV (Figure 2). The early pressure collapse implies rapid reaction kinetics and shorter acid penetration depth, characteristic of a transport-limited regime. The high reactivity of 15% HCl accelerated $CaCO_3$ dissolution near the inlet, leading to a rapid formation of dominant wormholes and early breakthrough. Although the acid effectively created a conductive channel, the resulting dissolution was less uniform, as supported by the post-acid core-end image showing a well-defined, localized flow path. This behavior aligns with previous studies (Nasr-El-Din et al., 2008; Al-Ghamdi et al., 2014), where higher acid concentrations increased face dissolution and reduced the efficiency ratio (PV_{bt} / ΔP□ax).

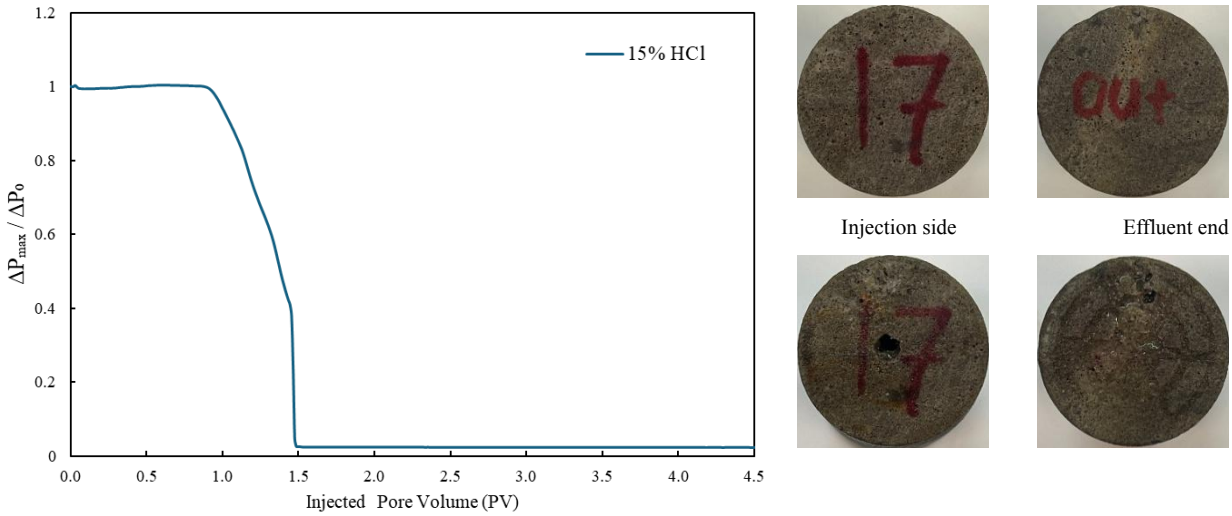

Fig. 2—Normalized differential pressure ($\Delta P_{max}/\Delta P_o$) versus injected pore volume for 15% HCl and corresponding core-end images before and after acidizing.

At the highest concentration tested (28% HCl, Core 12), the differential-pressure trend was notably unstable (Figure 3). While breakthrough theoretically occurred at 2.9 PV, acid injection was stopped at 2.3 PV due to rapid core damage and unstable flow behavior. The pressure curve exhibited multiple spikes followed by rapid drops, indicating alternating periods of pore plugging, localized dissolution, and wormhole collapse. The high acid strength caused an aggressive reaction near the inlet surface, generating CO_2 gas and fines migration that temporarily increased resistance before sudden pressure relief. Post-test imaging confirmed severe inlet corrosion and irregular dissolution, consistent with diffusion-limited, turbulent wormhole formation. Such behavior emphasizes that overly strong acids can result in inefficient matrix stimulation by consuming acid near the face before deep penetration. The performance of the green acid (Oil Safe AR®) (Core 1) paralleled that of the 15% HCl system but with a slightly higher PVbt of 1.54 PV (Figure 4). The pressure drop occurred more gradually, suggesting that the buffering additives effectively moderated the acid reactivity and reduced near-wellbore damage. The controlled dissolution pattern produced smoother flow channels and more uniform dissolution fronts, evident from the core-end morphology. Compared with 15% HCl, the green acid (Oil safe AR®) demonstrated a more desirable reaction rate, balancing acid effectiveness and penetration depth. This confirms that properly formulated organic-inhibited systems can serve as environmentally safer alternatives for carbonate stimulation, maintaining performance while minimizing corrosion and face damage.

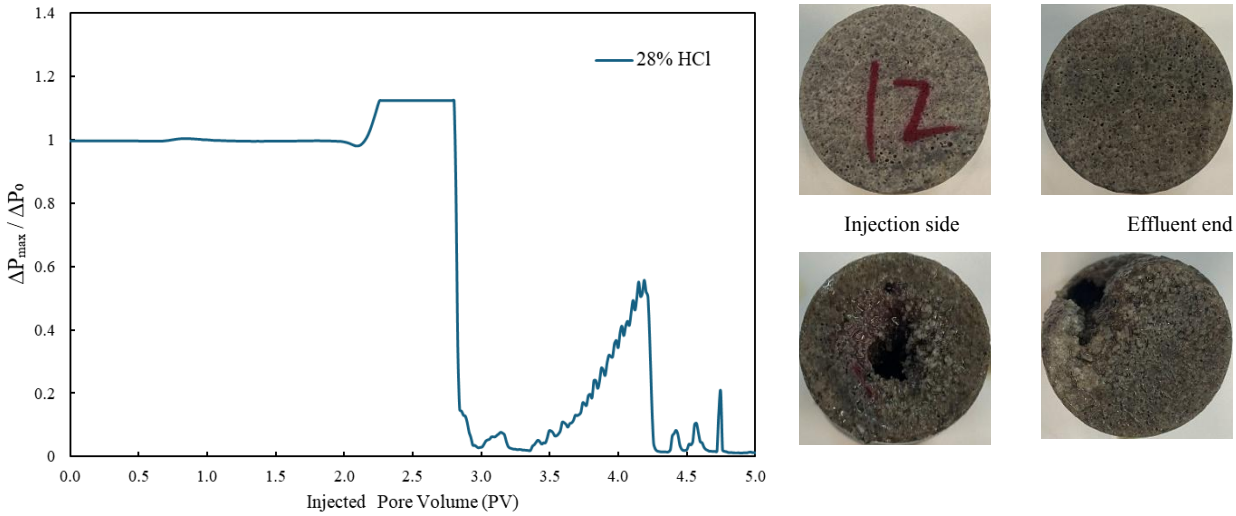

Fig. 3—Normalized differential pressure ($\Delta P_{max}/\Delta P_o$) versus injected pore volume for 28% HCl and corresponding core-end images before and after acidizing

3.1.2 Comparison and Interpretation of Acid Efficiency

A comparative summary of breakthrough parameters for all acid systems is presented in Table 2. The 7.5% HCl system required the largest PV_{bt} (2.55 PV), confirming slower reaction and deeper acid penetration, while the 15% HCl and green acid (Oil Safe AR®) achieved early breakthroughs (~1.5 PV). The 28% HCl system exhibited the least stable pressure response and the most aggressive

dissolution, confirming the detrimental effect of excessive acid strength on wormhole uniformity. Overall, the trend of PV_{bt} decreased with increasing acid concentration up to 15%, then increased at 28%, indicating an optimum concentration around 15% HCl for the tested cores. However, the green acid (Oil Safe AR®) achieved comparable breakthrough efficiency with improved operational safety, making it a promising candidate for field application. The post-acid brine injection segment in each test confirmed a substantial permeability increase, as reflected by the near-zero pressure differential after breakthrough. Visual inspection of the core ends (Figure 1-4) showed distinct dissolution morphologies: the 7.5% acid produced fine, homogeneous pores; 15% acid generated dominant central channels; 28% acid caused severe face etching and irregular wormhole branching; and the green acid (Oil Safe AR®) yielded a smooth, stable flow path. These observations collectively confirm that acid concentration and formulation strongly influence the dissolution mechanism, wormhole geometry, and overall stimulation efficiency in limestone formations.

Table 2 Summary of Single-Coreflood Experiments (40 °C, 1400 psi)

Acid Type	Core #	Porosity (%)	$K_{Initial}$ (md)	PV_{bt}
7.5% HCl	13	13.05	4.75	2.55 PV
15% HCl	17	15.6	2.76	1.48 PV
28% HCl	12	13.84	2.89	2.9 PV *
Green Acid	1	20.47	3.62	1.54 PV

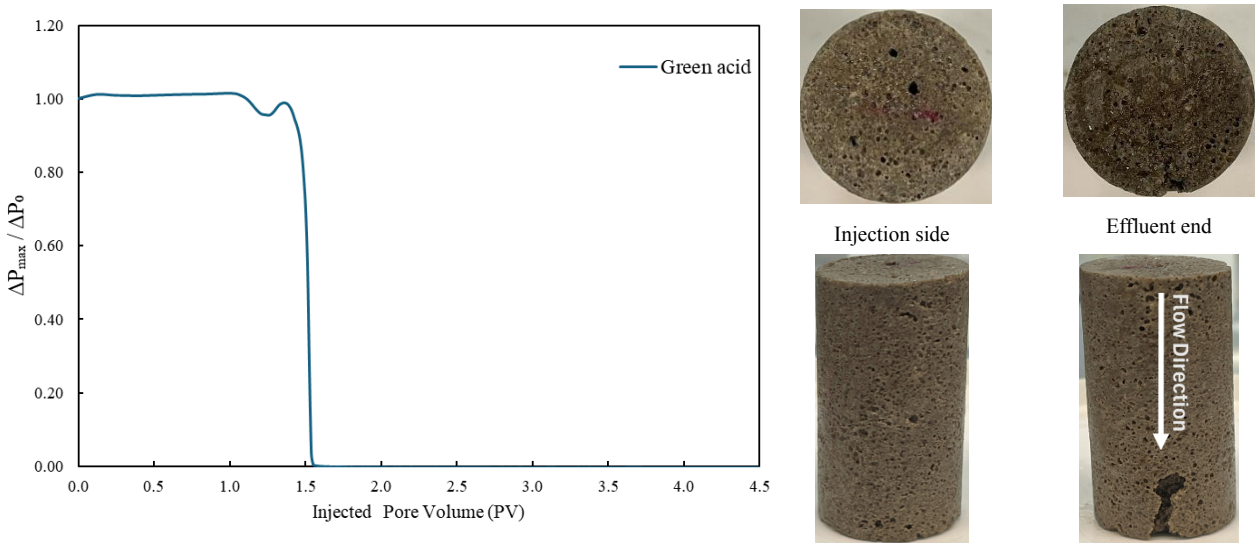

Fig. 4—Normalized differential pressure ($\Delta P_{max}/\Delta P_o$) versus injected pore volume for green acid and corresponding core-end images before and after acidizing

3.2 High-Temperature Dissolution Performance of Green Acid (Oil Safe AR®) vs. HCl

The high-temperature single-core experiments provide important insight into how dissolution regimes shift when acidizing is performed under thermally accelerated reaction conditions. Across all Oil Safe AR formulations, permeability-enhancement ratios ranged from 80 to 351, while the two 15 wt% HCl tests produced ratios of 363 and 68, depending on the initial core permeability (Table 3). This divergence between high- and low-permeability cores highlights a key mechanistic difference: while HCl maintains strong performance in tighter rocks because of its rapid reaction rate and strong face dissolution, it underperforms in higher-permeability substrates where the acid spends too quickly and fails to propagate deeply. In contrast, the moderated reaction kinetics of the green acid systems (Oil Safe AR®) enabled more consistent wormhole development independent of initial permeability. Breakthrough pore volumes for the green acid (Oil Safe AR®) ranged between 0.48 and 1.23 PV, similar to the 0.48–0.56 PV required for HCl but achieving more uniform and stable permeability increases. These observations align with earlier low-temperature findings and reinforce the conclusion that the synthetic acid system maintains controlled dissolution across a wider range of conditions. The results also demonstrate that green acid (Oil Safe AR®) avoids the excessive face dissolution and inlet damage commonly associated with HCl at elevated temperatures, producing more stable and sustainable conductivity improvements.

A reduced comparison focusing only on low- versus high-permeability conditions confirms this trend. Oil Safe AR 1060 produced enhancement factors of 351 (low perm) and 80 (high perm), whereas 15% HCl yielded 363 (low perm) and 68 (high perm) as shown in table 4. While both systems were effective in lower-permeability cores, the green acid (Oil Safe AR®) provided more balanced performance across permeability ranges. This behavior is particularly important for field applications, where heterogeneity and variable rock quality can compromise stimulation efficiency. The high-temperature data, therefore, demonstrate that the green acid

system (Oil Safe AR®) maintains its advantages in penetration depth, wormhole uniformity, and permeability retention even as temperature and reaction rates increase, making it a reliable alternative to traditional HCl acidizing under a broader set of reservoir conditions.

Table 3 — Baseline Comparison of Low- vs High-Permeability Performance at High Temperature

Core ID	Injectant	Flow rate (cc/min)	K_initial (md)	K_final (md)	K ratio	PV injected	PV at BT	Spent acid (PV)
L9	1060	4	37	12,992	351	14.92	15.69	0.77
L14	1050	4	42	13,717	327	30.15	30.86	0.71
L10	1030	4	41	11,118	271	23.70	24.93	1.23
L13	15% HCl	4	44	15,997	364	27.62	28.10	0.48
#5	15% HCl	4	160.5	10,967	68	24.42	24.98	0.56
#7	1060	4	169.89	13,556	80	24.56	25.78	1.22

Table 4 — Baseline Comparison of Low- vs High-Permeability Performance at High Temper

Acid System	Low-Perm Core (K ratio)	High-Perm Core (K ratio)
Oil Safe AR (1060)	351	80
15% HCl	363	68

3.3 Dual-core Acidizing Experiments at low temperature

The low-temperature dual-core coreflooding experiments, conducted at 40 °C, 1400 psi back pressure, 2500 psi confining pressure, and an injection rate of 3 cm³/min for approximately 650 s, reveal clear and systematic differences between the mineral-acid and green-acid systems (Oil Safe AR®) in terms of flow diversion, pressure evolution, and permeability enhancement. Despite the same nominal permeability contrast of 3.3:1 in both experiments, the pressure responses and dissolution patterns diverged substantially. In the 15 wt% HCl with surfactant system (A1) in Figure 5, the differential-pressure profiles across the low-permeability and high-permeability cores were nearly identical throughout acid injection, indicating that flow distribution remained controlled primarily by the intrinsic permeability contrast with minimal diversion. Only small fluctuations were observed in the ΔP signal before both cores experienced a rapid collapse in pressure at breakthrough, which is characteristic of HCl under low-temperature conditions, where its rapid reaction rate leads to aggressive inlet-face dissolution and preferential wormholing in the path of least resistance. Regained permeability measurements validate this interpretation: the low-permeability core showed only a modest increase (from 1.74 to 2.42 mD, ~39% improvement), whereas the high-permeability core exhibited an extreme increase (from 8.46 to 8918 mD), consistent with uncontrolled, highly localized dissolution and possible structural weakening rather than uniform, well-controlled wormhole development. Core-face photographs further revealed severe inlet etching, rough dissolution fronts, and non-uniform channeling typical of fast, highly reactive mineral-acid behavior in coreflood configurations.

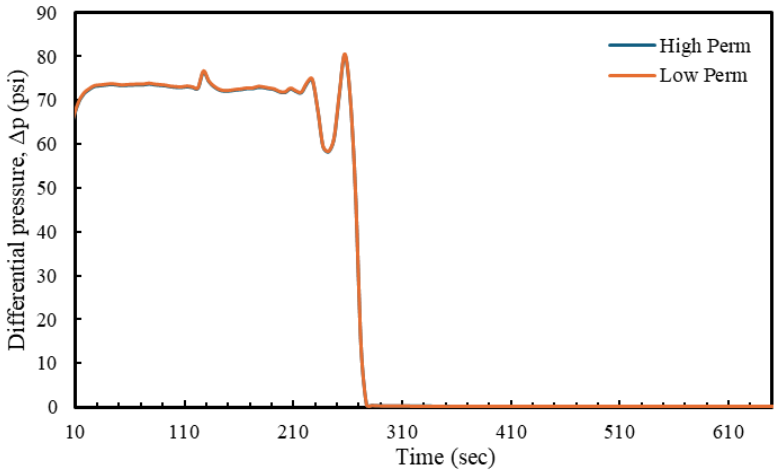

Fig. 5— Differential pressure versus time for the dual-core coreflood using 15 wt% HCl with surfactant at 40 °C

In contrast, the green-acid (Oil Safe AR®) with surfactant system (A2) demonstrated distinct pressure evolution and dissolution characteristics. Although the permeability contrast was identical (3.3:1), the absolute permeability of the low-permeability core in A2 was substantially tighter (0.50 md) than in A1 (1.74 md). Such a tight core typically suppresses diversion in controlled laboratory

corefloods, particularly at low temperature where micelle formation and in-situ viscosification proceed more slowly. Despite this more challenging configuration, the green-acid system (Oil Safe AR®) (Figure 6) produced a clear divergence in pressure response between the two cores. The low-perm core exhibited a continuously increasing differential-pressure profile, rising from ~160 psi at early injection to more than 350 psi just prior to breakthrough, while the high-perm core showed a more moderate and stable increase. This separation indicates that the green-acid (Oil Safe AR®) formulation temporarily increased resistance in the higher-permeability core, thereby redirecting fluid into the tighter core and demonstrating effective self-diverting behavior at the coreflooding scale. Regained permeability measurements support this mechanistic interpretation. The high-permeability core treated with green acid (Oil Safe AR®) exhibited a substantial enhancement (from 2.52 to 10,865.5 md), consistent with the formation of continuous and stable wormholes. Meanwhile, the low-permeability core displayed a controlled gain (from 0.50 to 0.63 md) without signs of collapse or uncontrolled dissolution. Core-face photographs revealed smoother dissolution fronts (see Appendix A), more continuous wormhole patterns. These observations collectively indicate that the moderated reaction kinetics of the green-acid system (Oil Safe AR®) promote deeper penetration, more uniform dissolution, and robust flow diversion even under low-temperature conditions that typically limit in-situ surfactant structuring.

Table 5 — Summary of dual-core coreflooding results at 40 °C

Acid System	Core Type	Initial k (mD)	Regained k (mD)	k Increase (%)
15% HCl + surfactant (A1)	Low perm	1.74	2.42	+39%
	High perm	8.46	8918	Very large
Green Acid + surfactant (A2)	Low perm	0.50	0.63	+26%
	High perm	2.52	10,865.5	Very large

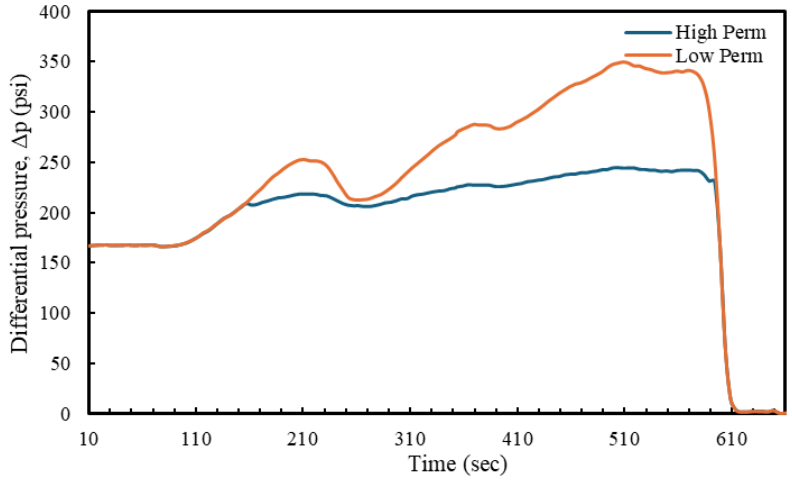

Fig. 6— Differential pressure versus time for the dual-core coreflood using green acid with surfactant at 40 °C

The high-temperature dual-core coreflooding experiments conducted at 82 °C reveal important differences in how green-acid (Oil Safe AR®) and HCl systems distribute flow and generate wormhole networks when the acid–carbonate reaction is thermally accelerated. In the green-acid (Oil Safe AR®) test performed at 4 cm^3/min (Test 6–H30), a clear divergence in differential-pressure behavior was observed between the high-permeability and low-permeability cores, indicating that the acid preferentially entered the tighter pathway despite an initial permeability ratio of 7.7. The low-permeability core exhibited a sustained differential-pressure buildup followed by significant permeability enhancement from 51.6 md to 11,733 md, while the high-permeability core increased from 399.8 md to 8503 md. This shift reduced the dual-core permeability ratio from 7.7 to 0.7, confirming strong diversion. The breakthrough at ~1.89 PV and intermediate spent-acid fraction reflect deeper and more uniformly distributed dissolution consistent with moderated reaction kinetics at elevated temperature. The differential-pressure trend for this experiment is shown in Figure 7, and the corresponding permeability metrics are summarized in Table 6. The inlet and outlet photographs for this green-acid (Oil Safe AR®) test show smoother dissolution fronts, more continuous wormhole structures, and minimal face damage, as illustrated in Figure 8.

Table 6 — Summary of High-Temperature Dual-Core Coreflood Results.

Test Pair	Injectant	Flow Rate (cc/min)	Initial k Ratio	Final k Ratio	Breakthrough (PV)	Spent Acid (PV)

#6 – H30	1060	4	7.7	0.7	1.89	0.54
#4 – H4	15% HCl	4	7.4	2.6	1.53	0.31

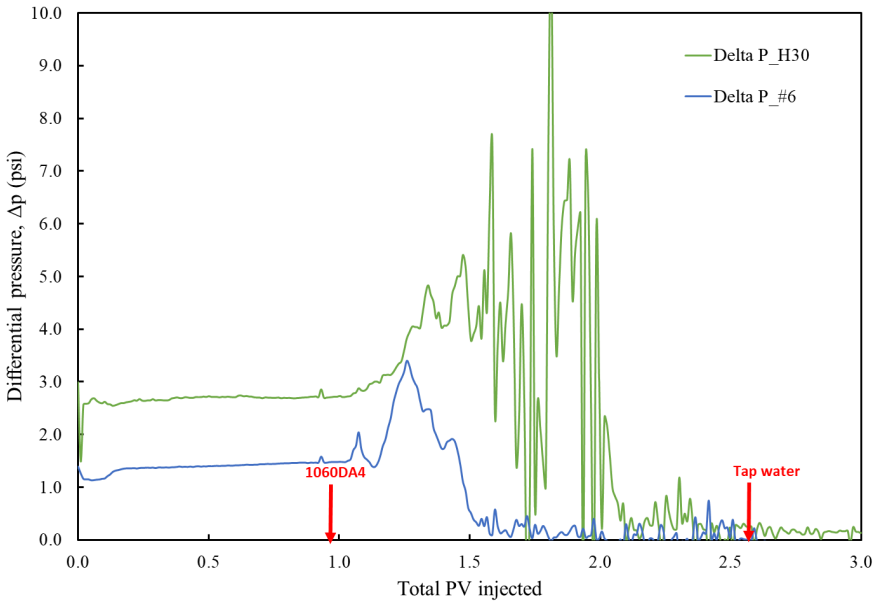

Fig. 7— Differential pressure versus Total pore volume injected for green acid at 4 cm³/min and 82 °C

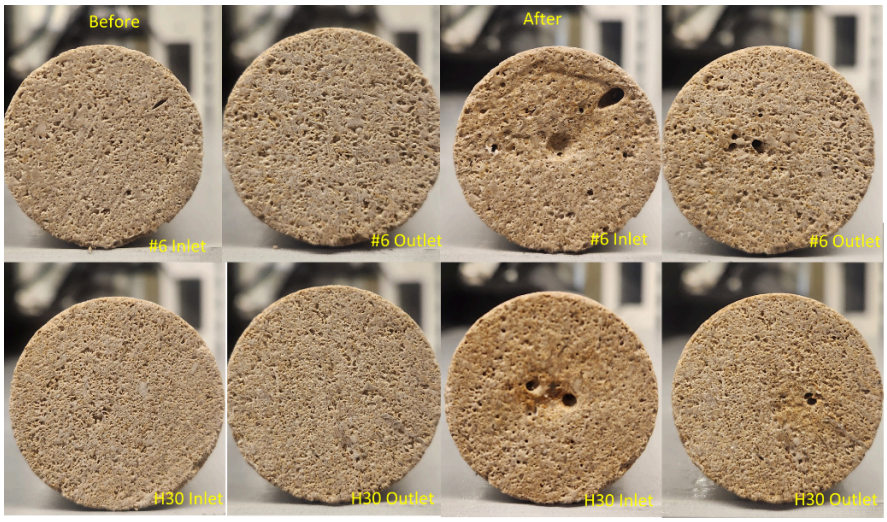

Fig. 8— Green Acid Test at 4 cm³/min and 82 °C (Test 6–H30) core-face photographs: inlet and outlet, pre- and post-acidizing.

The 15 wt% HCl test conducted at the same flow rate of 4 cm³/min (Test 4–H4) also exhibited diversion, although the effect was less stable and more transient compared with the green-acid system (Oil Safe AR®). In this case, the low-permeability core experienced a noticeable pressure-rise phase before breakthrough, indicating temporary flow redistribution, but dissolution soon became dominated by the high-permeability pathway. The dual-core permeability ratio shifted from 7.4 to 2.6, and both cores showed substantial permeability increases, with the low-perm core rising from 42.7 md to 8980 md and the high-perm core from 314.2 md to 23,140 md. The differential-pressure behavior in Figure 9 reflects the rapid reaction kinetics of HCl at elevated temperature, which can briefly impose resistance in the high-perm core but ultimately generates a dominant wormhole that suppresses sustained diversion. Compared with the green-acid (Oil Safe AR®) case, the HCl system displayed more aggressive inlet-face dissolution and a less uniform wormhole network, as evidenced by the inlet and outlet core-face photographs shown in Figure 10. The permeability outcomes for this experiment are provided in Table 6, further confirming that diversion with HCl under high-temperature conditions is short-lived and dominated by fast, localized dissolution.

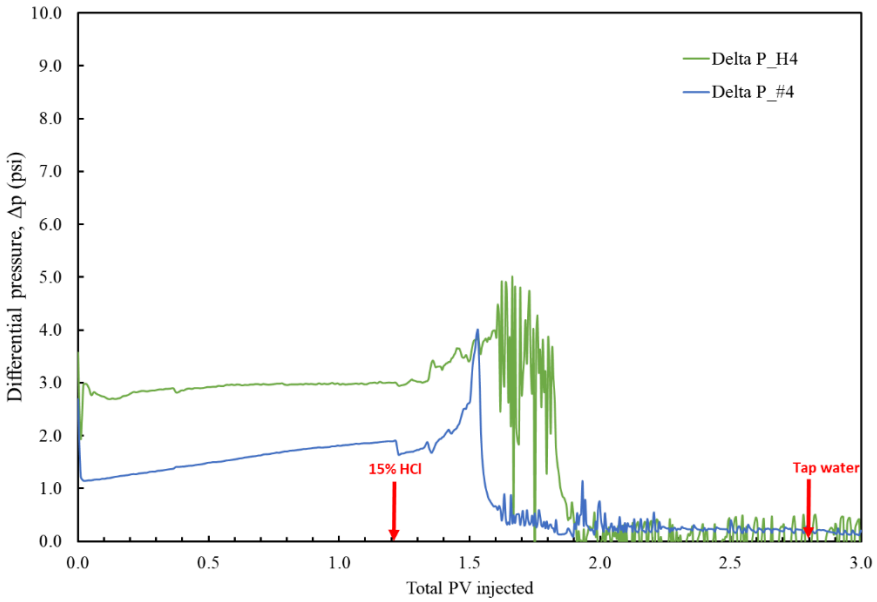

Fig. 9— Differential pressure versus Total pore volume injected for 15% HCl at 4 cm³/min and 82 °C

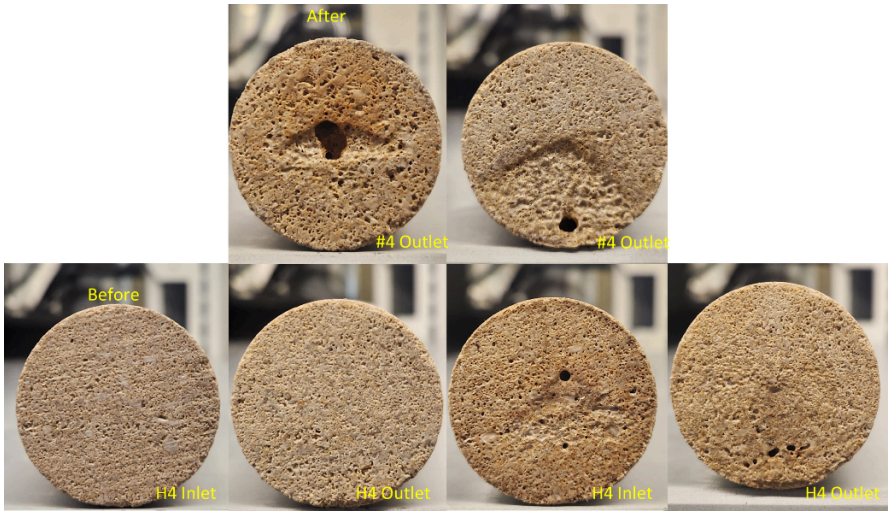

Fig. 10— 15% HCl Test at 4 cm³/min and 82 °C (Test 4 – H4) core-face photographs: inlet and outlet, pre- and post-acidizing.

4. Field Case Study: Evaluation of Green Acid (Oil Safe AR®) Performance in Production and Injection Wells

To complement the laboratory scale coreflooding results and demonstrate the applicability of the green acid system (Oil Safe AR®) under real operating conditions, a collection of field treatments from various producing and injection wells was analyzed. These wells differ in permeability, stimulation history, operational age, and near wellbore damage severity, providing a representative dataset for assessing acid performance in diverse reservoir environments. The field outcomes show clear and consistent improvements in well performance following treatment with the synthetic green acid Oil Safe AR®), with producing wells exhibiting substantial increases in hydrocarbon rate and injection wells showing strong and sustained enhancement in injectivity. Table 7 summarizes typical responses for oil producing wells, while Figure 11 illustrates the post-stimulation production profile for a representative case, showing a stabilized rate that remained 100–150 times higher than the original baseline. For instance, A formation increases from 0.03 m^3/d to 4.5 m^3/d. Other formations demonstrated three to four-fold improvements. These results reveal that the green acid system (Oil Safe AR®) effectively restores flow capacity and reduces near-wellbore skin without requiring aggressive acid concentrations. Importantly, the persistence of these improvements over periods of three months or longer indicates that the treatment creates deeper, more conductive dissolution pathways rather than providing a short-term perforation cleanup, directly supporting the laboratory findings on moderated reaction kinetics and controlled wormhole development.

Table 7 — Oil Well Responses to Green Acid Treatment

Well	Formation	Treatment volume (m^3/m)	Pre-Stimulation Production (production per day)	Production After Treatment (production per day)	Increase in Oil Production (%)

1	A	1	0.03 m^3 Oil and 0.02 m^3 H_2O average / day	4.5 m^3 Oil and 7.5 m^3 H_2O average/day after 3 months	Large
2	B	1	0.5 m^3 Oil average/day	2.0 m^3 Oil average/day	300%
3	C	1	0.3 m^3 oil and 0.2 m^3 H_2O average/day	1 m^3 Oil and 1.5 m^3 H_2O average/day	230%
4	D	1	0.08 m^3 Oil and 0.05 m^3 H_2O average/day	1.7 m^3 Oil and 2.0 m^3 H_2O average/day	Large

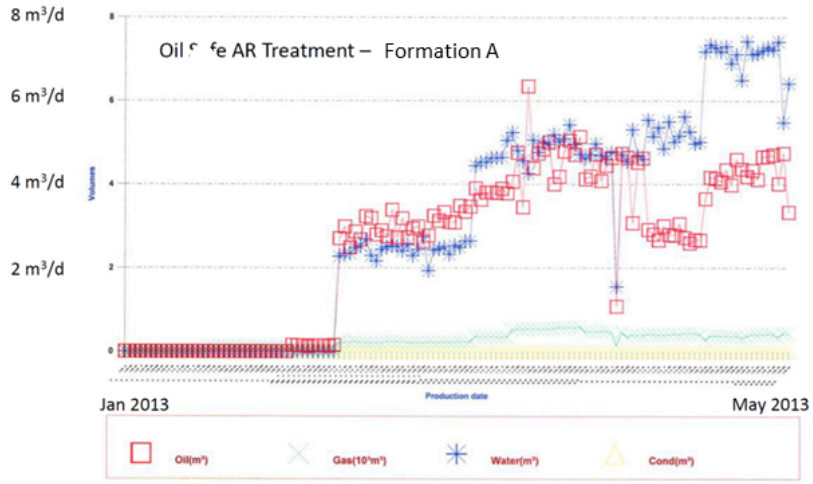

Fig. 11— Representative production profile response following green acid treatment

The scientifically significant outcome from these producing-well treatments is the convergence between measured field responses and the dissolution behavior observed in controlled coreflood experiments. The laboratory results demonstrated that the green acid system (Oil Safe AR®) possesses a linear, moderated spending rate that allows deeper penetration into carbonate matrices before complete reaction, enhancing the extent of stimulated rock volume. This behavior contrasts sharply with traditional hydrochloric acid, which reacts extremely rapidly at the rock face, often causing premature face dissolution, near-wellbore collapse, and limited wormhole extension. The field results support this mechanistic interpretation: wells treated with the green acid (Oil Safe AR®) exhibit not only immediate rate increases but also long-term stability, indicating that the acid created extended conductive channels instead of shallow dominant wormholes. Furthermore, the built-in surfactant, iron-control, and mild corrosion-inhibitor components within the green acid (Oil Safe AR®) formulation minimize the formation of sludge, emulsions, and precipitates, reducing the likelihood of secondary formation damage that might otherwise cause rapid post-treatment decline. This alignment between laboratory and field behavior strengthens the conclusion that the green acid system Oil Safe AR®) can provide stimulation efficiency comparable to or greater than conventional HCl while significantly reducing operational risks.

4.2 Gas-Production Case Responses

The field data also includes multiple gas producing wells treated with the same green acid system (Oil Safe AR®). As summarized in Table 8, the observed increases in gas production ranged from 188% to more than 250% relative to baseline conditions, with some wells transitioning from marginal or uneconomic production to stable, higher volume operation. Figure 12 provides a representative example of the production rate trend after treatment. Gas wells serve as particularly useful indicators of stimulation success because gas deliverability is highly sensitive to skin, near-wellbore tortuosity, and residual damage from drilling fluids or fines migration. The substantial and sustained improvements observed across multiple cases suggest that the green acid (Oil Safe AR®) effectively removed long-standing damage and restored permeability in the fracture-network and matrix regions immediately surrounding the wellbore. Consistent with laboratory coreflood data, the moderated reactivity of the green acid (Oil Safe AR®) likely allowed it to penetrate deeper before spending, thus contacting previously unstimulated pore systems and improving overall transmissibility. The absence of post-treatment decline in the field data further suggests minimal precipitation, low risk of fines destabilization, and efficient cleanup, all properties supported by the environmentally benign chemistry of the green acid system (Oil Safe AR®).

Table 8 — Gas Well Responses to Green Acid Treatment Oil Safe AR Case Study Data

Well	Formation	Treatment volume (m^3/m)	Pre-Stimulation Production (production per day)	Production After Treatment (production per day)	Increase in Gas Production (%)
1	E	10 m^3 into horizontal	Hz scaled off, well shut in – uneconomic to produce	17 ×10³ m^3/d gas, 2.5 m^3/d condensate, 17 m^3/d H_2O	Large

2	F	1	2 ×10³ m³/d	7 ×10³ m³/d	250%
3	G	0.5	2.5 ×10³ m³/d	9.0 ×10³ m³/d	260%
4	H	1	1.6 ×10³ m³/d	4.6 ×10³ m³/d	188%

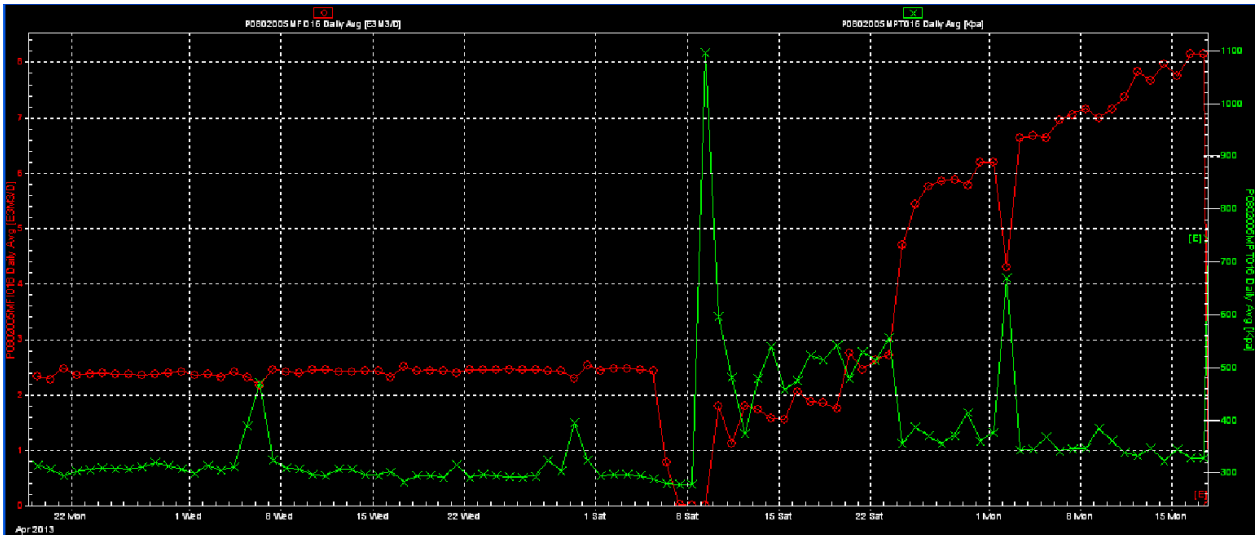

Fig. 12— Representative Gas-Rate Response Following Green Acid Treatment

Conclusion

This study demonstrated that the synthetic green-acid formulation (Oil Safe AR®) provides a controlled and efficient alternative to conventional 15 wt% HCl for matrix acidizing in carbonate systems across a wide range of temperatures and permeability conditions. Single-core experiments confirmed that green acid (Oil Safe AR®) produces significant permeability enhancement through moderate reaction kinetics that promote deeper acid penetration and avoid the severe inlet-face dissolution characteristic of mineral acid. Dual core coreflooding at low temperature further showed that the green acid (Oil Safe AR®) is capable of generating stable diversion even when the absolute permeability of the tighter core is extremely low, redirecting flow and producing uniform wormhole networks, whereas HCl displayed minimal and short-lived diversion under the same conditions. At high temperature, the diversion performance of both acids became more sensitive to flow rate. Green acid (Oil Safe AR®) achieved strong diversion at sufficiently high injection velocity, reducing the dual-core permeability ratio from 7.7 to 0.7, while HCl produced only transient flow redistribution before reverting to preferential dissolution in the more permeable core. These findings highlight that the controlled reactivity of the green acid (Oil Safe AR®) contributes to sustained diversion and balanced dissolution in thermally accelerated environments. Field-treatment data supported the laboratory observations, demonstrating consistent improvements in post-stimulation productivity and injectivity that persisted over extended operational periods.

References

Alameen, M. B., Elraies, K. A., Almansour, A., Mohyaldinn, M., & Hagar, H. (2023). Quartz Hydrolysis Analysis of Pure Quartz for Enhanced Oil Production; Influence of Time, pH, and Salinity on Hydrolysis. *Journal of Advanced Research in Fluid Mechanics and Thermal Sciences*, *111*(2), 99–106. https://doi.org/10.37934/ARFMTS.111.2.99106

Alameen, M. B., Elraies, K. A., Mohyaldinn, M., Almansour, A., Gmail, A. M., & Hagar, H. (2024). Reducing the Sand Production from Semi-Consolidated Sandstone Formation by Mitigating the Silica Dissolution Factor During Water Breakthrough. *International Petroleum Technology Conference, IPTC 2024*, 12–14. https://doi.org/10.2523/IPTC-23402-EA

Al-Ghamdi, A. H., Mahmoud, M. A., Wang, G., Hill, A. D., & Nasr-El-Din, H. A. (2014). Acid Diversion by Use of Viscoelastic Surfactants: The Effects of Flow Rate and Initial Permeability Contrast. *SPE Journal*, *19*(06), 1203–1216. https://doi.org/10.2118/142564-PA

Alhubail, M. M., Misra, A., & Barati, R. (2017). A Novel Acid Transport Model with Robust Finite Element Discretization. *Society of Petroleum Engineers - SPE Kingdom of Saudi Arabia Annual Technical Symposium and Exhibition 2017*, 1453–1469. https://doi.org/10.2118/188030-MS

Alhubail, M. M., Misra, A., Maulianda, B., & Barati, R. (2020). Application of finite element discretization with weak formulation for simulation of acid fracturing in tight carbonate reservoirs. *Journal of Petroleum Science and Engineering*, *190*, 107047. https://doi.org/10.1016/J.PETROL.2020.107047

Ali, M. T., Aziz Ezzat, A., & Nasr-El-Din, H. A. (2020). A model to simulate matrix-acid stimulation for wells in dolomite reservoirs with vugs and natural fractures. *SPE Journal*, *25*(2), 609–631. https://doi.org/10.2118/199341-PA

Ali, M. T., & Nasr-El-Din, H. A. (2020). New insights into carbonate matrix acidizing treatments: A mathematical and experimental study. *SPE Journal*, *25*(3), 1272–1284. https://doi.org/10.2118/200472-PA

Aljawad, M. S., Aboluhom, H., Schwalbert, M. P., Al-Mubarak, A., Alafnan, S., & Mahmoud, M. (2021). Temperature impact on linear and radial wormhole propagation in limestone, dolomite, and mixed mineralogy. *Journal of Natural Gas Science and Engineering*, *93*. https://doi.org/10.1016/J.JNGSE.2021.104031

Barati Ghahfarokhi, Reza., & Alhubail, M. Makki. (2021). *Unconventional hydrocarbon resources : techniques for reservoir engineering analysis*. 584. https://www.wiley.com/en-us/Unconventional+Hydrocarbon+Resources%3A+Techniques+for+Reservoir+Engineering+Analysis-p-9781119420675

Barati Ghahgarokhi, R., Alhajeri, M. M., Tsau, J. S., & Rowley, S. (2024). Green Acid (Oil Safe AR®) Transformative Technology for Sustainable Oil Production, Reservoir Management and Operational Efficiency in UAE Hydrocarbon Recovery. *Society of Petroleum Engineers - ADIPEC 2024*. https://doi.org/10.2118/222022-MS

Barboza, R. P., Schwalbert, M. P., Favero, J. L., Dias, R. A. C., Moraes, A. O. S., Silva, L. F. L. R., & Thompson, R. L. (2022). Modeling and simulation of the carbonate reactive-dissolution process by viscoelastic-surfactant-based acid. *Journal of Petroleum Science and Engineering*, *215*. https://doi.org/10.1016/J.PETROL.2022.110595

Bazin, B. (2001). From matrix acidizing to acid fracturing: A laboratory evaluation of acid/rock interactions. *SPE Production and Facilities*, *16*(1), 22–29. https://doi.org/10.2118/66566-PA

Cao, C., Zhou, F., Cheng, L., Liu, S., Lu, W., & Wang, Q. (2021). A comprehensive method for acid diversion performance evaluation in strongly heterogeneous carbonate reservoirs stimulation using CT. *Journal of Petroleum Science and Engineering*, *203*. https://doi.org/10.1016/J.PETROL.2021.108614

Cao, X., Sun, Y., Sun, Y., Xie, D., Li, H., & Liu, M. (2021). Conductive halloysite clay nanotubes for high performance sodium ion battery cathode. *Applied Clay Science*, *213*. https://doi.org/10.1016/j.clay.2021.106265

Dong, K. (2018). A new wormhole propagation model at optimal conditions for carbonate acidizing. *Journal of Petroleum Science and Engineering*, *171*, 1309–1317. https://doi.org/10.1016/J.PETROL.2018.08.055

Golfier, F., Zarcone, C., Bazin, B., Lenormand, R., Lasseux, D., & Quintard, M. (2002). On the ability of a Darcy-scale model to capture wormhole formation during the dissolution of a porous medium. *Journal of Fluid Mechanics*, *457*, 213–254. https://doi.org/10.1017/S0022112002007735

Hagar, H. S., Alshatti, H., Alhajeri, M. M., Tsau, J.-S., Glatz, G., & Barati, R. (2025). Geochemical Controls on Organic and Inorganic Scale Deposition: Insights from CO2 Injection in Morrow Fluvial Sandstone. *ADIPEC*. https://doi.org/10.2118/229892-MS

Hagar, H. S., Forooezsh, J., Zivar, D., Kumar, S., Abdulelah, H., & Dzulkarnain, I. B. (2020). Simulation of Hydrogen Sulfide Generation in Oil and Gas Geological Formations. *2020 International Conference on Computational Intelligence (ICCI)*, 121–125. https://doi.org/10.1109/icci51257.2020.9247695

Hagar, H. S., & Foroozesh, J. (2021). Effect of CO2 and salinity on microbial hydrogen sulphide generation in hydrocarbon reservoirs. *Journal of Natural Gas Science and Engineering*, *96*, 104288. https://doi.org/10.1016/j.jngse.2021.104288

Hagar, H. S., Foroozesh, J., Kumar, S., Zivar, D., Banan, N., & Dzulkarnain, I. (2022). Microbial H2S generation in hydrocarbon reservoirs: Analysis of mechanisms and recent remediation technologies. *Journal of Natural Gas Science and Engineering*, 104729.

Hagar, H. S., Jufar, S. R., Foroozesh, J., Lee, J. H., Al-mahbashi, N., Alakbari, F. S., Jagaba, A. H., & Kwon, S. (2024). A sustainable chitin nanocrystal-stabilised emulsions to enhance the conformance control in porous media. *Colloids and Surfaces A: Physicochemical and Engineering Aspects*, *688*, 133591. https://doi.org/10.1016/J.COLSURFA.2024.133591

Hagar, H. S., Jufar, S. R., Lee, J. H., Al-mahbashi, N., Alameen, M. B., Kwon, S., Jagaba, A. H., & Rathnayake, U. (2023). Chitin nanocrystals: A promising alternative to synthetic surfactants for stabilizing oil-in-water emulsions. *Case Studies in Chemical and Environmental Engineering*, *8*, 100503. https://doi.org/10.1016/J.CSCEE.2023.100503

International Energy Agency (IEA). (2019). *World Energy Outlook 2019 – Analysis - IEA*. World Energy Outlook 2019. https://www.iea.org/reports/world-energy-outlook-2019

Liu, N., & Liu, M. (2016). Simulation and analysis of wormhole propagation by VES acid in carbonate acidizing. *Journal of Petroleum Science and Engineering*, *138*, 57–65. https://doi.org/10.1016/J.PETROL.2015.12.011

Liu, P., Li, J., Sun, S., Yao, J., & Zhang, K. (2021). Numerical investigation of carbonate acidizing with gelled acid using a coupled thermal–hydrologic–chemical model. *International Journal of Thermal Sciences*, *160*. https://doi.org/10.1016/J.IJTHERMALSCI.2020.106700

Ma, G., Chen, Y., Jin, Y., & Wang, H. (2018). Modelling temperature-influenced acidizing process in fractured carbonate rocks. *International Journal of Rock Mechanics and Mining Sciences*, *105*, 73–84. https://doi.org/10.1016/J.IJRMMS.2018.03.019

Maheshwari, P., Maxey, J., & Balakotaiah, V. (2016). Reactive-dissolution modeling and experimental comparison of wormhole formation in carbonates with gelled and emulsified acids. *SPE Production and Operations*, *31*(2), 103–119. https://doi.org/10.2118/171731-PA

Mahmoud, M., Kamal, M. S., Aljawad, M. S., Ali, A., & Al-Nakhli, A. (2021). Single-stage stimulation of anhydrite-rich carbonate rocks using chelating agent: An experimental and modeling investigation. *SPE Journal*, *26*(3), 1144–1160. https://doi.org/10.2118/203840-PA

Markey, F., Betz, T., Gauteplass, J., Taylor, K., Ackwith, D., & Barati, R. (2014). Examining Innovative Techniques For Matrix Acidizing In Tight Carbonate Formations To Minimize Damage To Equipment And Environment. *Society of Petroleum Engineers - SPE/AAPG/SEG Unconventional Resources Technology Conference*. https://doi.org/10.15530/URTEC-2014-1935101

Mohsin Yousufi, M., bin Dzulkarnain, I., Eissa Mohyaldinn Elhaj, M., binti Sufian, S., Mamo Negash, B., Salah Hagar, H., & Ahmed, S. (2025). Evaluation of activated carbon as a Pickering emulsion Stabilizer for conformance control at high temperature and Salinity: A Focus on stability and rheology. *Journal of Molecular Liquids*, *419*, 126764. https://doi.org/10.1016/J.MOLLIQ.2024.126764

Mustafa, A., Aly, M., Aljawad, M. S., Dvorkin, J., Solling, T., & Sultan, A. (2021). A green and efficient acid system (Oil Safe AR®)for carbonate reservoir stimulation. *Journal of Petroleum Science and Engineering*, *205*. https://doi.org/10.1016/J.PETROL.2021.108974

Nawik, A., Taylor, K., & Ghahfarokhi, R. B. (2016). An Environmentally Friendly Alternative for the Conventional Acids Used in Acid Fracturing of Carbonate Reservoirs. *Proceedings of the International Conference on Offshore Mechanics and Arctic Engineering - OMAE*, *8*. https://doi.org/10.1115/OMAE2016-54487

Zhang, L., He, J., Wang, H., Li, Z., Zhou, F., & Mou, J. (2021). Experimental investigation on wormhole propagation during foamed-VES acidizing. *Journal of Petroleum Science and Engineering*, *198*. https://doi.org/10.1016/J.PETROL.2020.108139

Zhu, D., Wang, Y., Cui, M., Zhou, F., Zhang, Y., Liang, C., Zou, H., & Yao, F. (2022). Effects of spent viscoelastic-surfactant acid flow on wormholes propagation and diverting performance in heterogeneous carbonate reservoir. *Energy Reports*, *8*, 8321–8332. https://doi.org/10.1016/J.EGYR.2022.06.056

Appendix

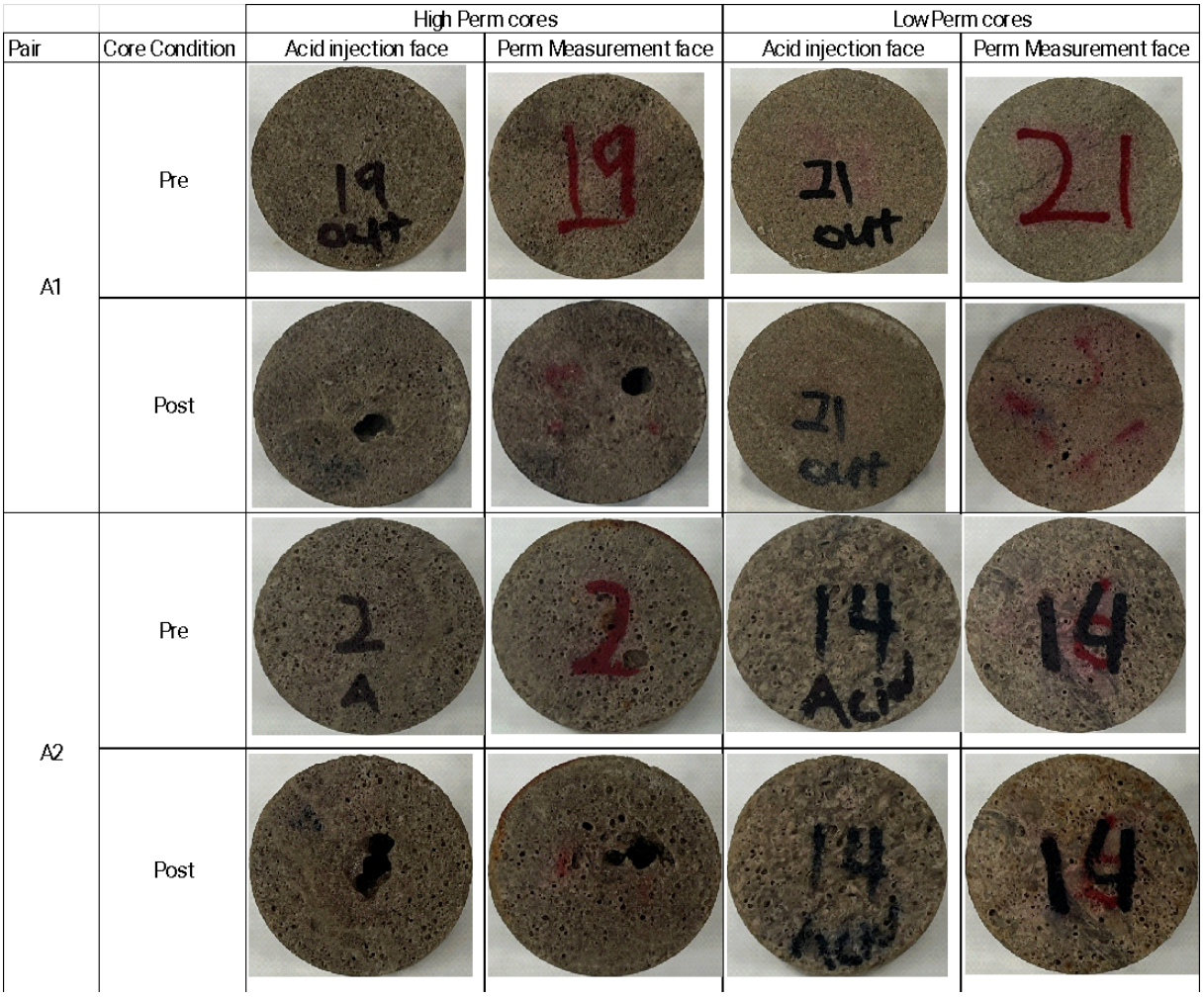

Fig. A-1—Pre- and post-acidizing inlet and outlet core-face photographs for the low-temperature (40°C) dual-core tests using green acid and 15 wt% HCl.